JOURNAL OF ACOUSTICS AND VIBRATION RESEARCH (JAVR)
ISSN: XXXX-XXXX
VOL. 4, ISSUE 1, 32 – 41

Identification of Suitable Excitation Nodes for Assembled Structures using Modal Participation Factors

M.S.A. Mohd Kahar[1], N.F.H. Ah Siak[1], M.A. Yunus[1], M.S.M Sani[2,3], W.I.I Wan Iskandar Mirza[4], M.A. Rahim[5], and M.N. Abdul Rani[1*]

[1]Structural Dynamics Analysis & Validation (SDAV),
Faculty of Mechanical Engineering, Universiti Teknologi MARA (UiTM),
Shah Alam, Selangor, Malaysia.
[2]Center for Automotive Engineering, Universiti Malaysia Pahang Al Sultan Abdullah,
26600 Pekan, Pahang, Malaysia
[3]Faculty of Mechanical and Automotive Engineering Technology, Universiti Malaysia Pahang Al Sultan Abdullah, 26600 Pekan, Pahang, Malaysia.
[4]Jabatan Kejuruteraan Mekanikal Kejituan (MPE), Malaysia-Japan International Institute of Technology (MJIIT), Universiti Teknologi Malaysia (UTM), Kuala Lumpur
[5]Fakulti Kejuruteraan & Teknologi Elektrik, Kampus Pauh Putra,
Universiti Malaysia Perlis, 02600 Arau, Malaysia

[*]Corresponding email: mnarani@uitm.edu.my

ABSTRACT

Accurate excitation point selection is essential in experimental modal analysis (EMA) to ensure sufficient excitation of structural vibration modes and the acquisition of quality Frequency Response Functions (FRFs). However, excitation nodes are commonly selected based on geometric accessibility and engineering judgement, which may result in incomplete dynamic characteristics. This study presents a systematic methodology for identifying suitable excitation nodes for a simplified aircraft structure. FE modal analysis is first performed using MSC NASTRAN SOL103 to obtain the eigenvalues and eigenvectors of the structure. The extracted modal parameters are subsequently used to calculate the Modal Participation Factors (MPFs) and effective modal masses for all candidate excitation nodes. Based on the obtained MPFs, excitation nodes are ranked according to their capability to excite multiple structural modes within the investigated frequency range. The effectiveness of the selected excitation locations is then validated using driving point FRF analysis through MSC NASTRAN SOL111. The results show that nodes with large MPF and effective modal mass values produce significantly stronger FRF amplitudes and clearer resonance peaks across multiple vibration modes. The strong agreement between the MPF based excitation ranking and the corresponding FRF responses demonstrates the effectiveness of the proposed methodology for EMA and structural dynamic investigations.

Article History

Received: 09/01/2026

Revised: 30/03/2026

Accepted: 15/05/2026

Published: 17/06/2026

Keywords: Modal Participation Factor; Frequency Response Function; Excitation Node; Eigenvalues; Eigenvectors

INTRODUCTION

Assembled structures are widely used in aerospace, automotive, marine, and mechanical engineering applications due to their manufacturing flexibility, maintainability, and structural efficiency. However, the dynamic behaviour of such structures is strongly influenced by the interaction between coupled substructures, particularly at the joint and interface regions [1-6] . Therefore, accurate identification of the dynamic characteristics of assembled structures is essential for vibration prediction, structural health monitoring, model validation, and FE model updating.

In EMA and FRF measurement, the selection of excitation location plays a critical role in determining the quality and completeness of the identified dynamic response [7-9]. An inappropriate excitation point may lead to insufficient modal participation, weak structural response, low signal to noise ratio, and incomplete identification of vibration modes [7, 10, 11]. Excitation applied near modal nodal regions can significantly suppress the contribution of specific modes, causing inaccurate estimation of resonance frequencies, damping ratios, and mode shapes.

The identification of suitable excitation points becomes considerably more challenging in assembled structures because the dynamic response is governed not only by the global structural modes but also by the local interaction behaviour at the interfaces and connection regions [8, 10, 11]. Joint flexibility, contact nonlinearity, and non-uniform stiffness distribution may alter the modal energy distribution and vibration transmission paths throughout the assembly [9, 12]. Consequently, excitation locations that are effective for individual substructures may become ineffective after assembly due to mode coupling and interface induced dynamic modifications.

Existing excitation point selection approaches are commonly based on engineering experience, geometric accessibility, or trial and error procedures [2, 13-16]. Several studies have proposed sensor and excitation optimisation techniques using modal kinetic energy, effective independence, or modal assurance criteria [10, 17, 18]. However, most existing methods primarily focus on monolithic components or structures and often neglect the influence of interface dynamics and coupling effects inherent in assembled systems. As a result, the selected excitation locations may not provide sufficient excitation efficiency across all dominant modes of the assembled structure.

This study presents a systematic methodology for identifying suitable excitation points for assembled structures based on MPFs and FRF behaviour [7, 8]. The proposed approach evaluates the excitation effectiveness of candidate locations by considering modal controllability, response amplitude distribution, and multi mode excitation capability. The methodology is applied to an assembled structural system represented by a simplified aircraft structure to identify excitation locations capable of producing representative and useful information dynamic responses for EMA and model validation purposes. The proposed methodology improves the reliability of EMA for assembled structures and provides a more systematic basis for excitation point selection in structural dynamics applications involving coupled and interface dominated systems.

METHODOLOGY

This section presents the methodology adopted in this study. In the first stage, the FE modal analysis is performed using MSC NASTRAN SOL103 to determine eigenvalues and eigenvectors of the simplified aircraft. In the second stage, Modal Participation Factors (MPFs) are calculated from the obtained eigensolutions to quantify the contribution of each candidate excitation point to the excitation of the structural modes. In the final stage, the effectiveness of the selected excitation points is evaluated using MSC SOL111, allowing MPF based predictions to be verified through the resulting FRFs.

FE Modelling of the Simplified Aircraft

The FE model of the simplified aircraft consists of six substructures namely one fuselage, two wings, two horizontal stabilisers and one vertical stabiliser as shown in Figure 1.

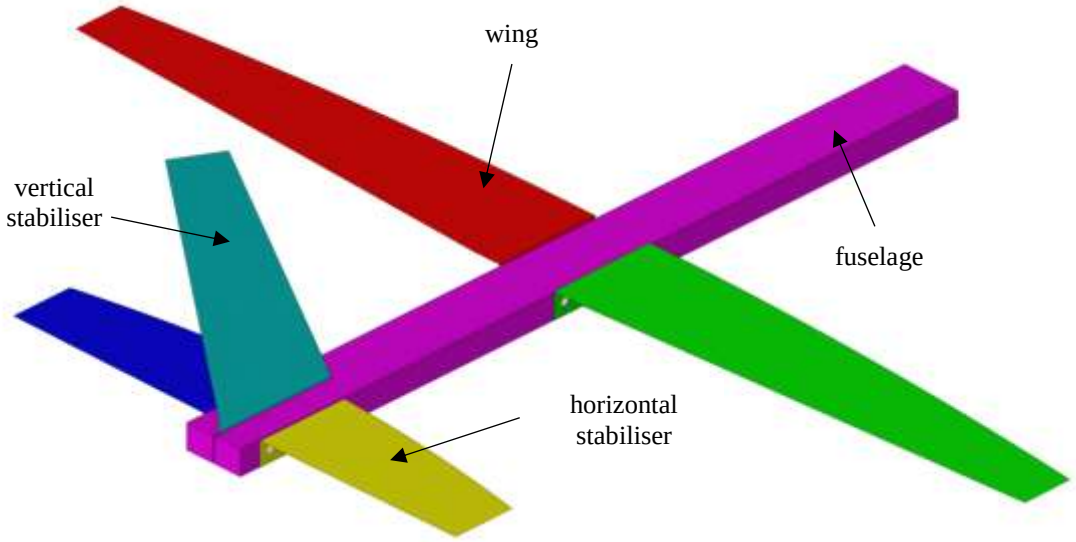

Figure 1: FE model of the simplified aircraft

Meshing of the fuselage was carried out using volumetric tetrahedral elements with R-Tria meshing, while 2D triangular shell elements were used for the wings, horizontal stabilisers and vertical stabilisers. RBE2-spider approach was used to couple the substructures. The use of these element types, which are commonly adopted in structural vibration analysis, enables improved representation of local stiffness distribution while maintaining a balanced element count and computational efficiency. Material properties were defined as shown in the Table 1, assuming uniform aluminium throughout the models. Young's modulus was set to $E = 72000$ MPa, Poisson's ratio to $\nu = 0.3$ and the density was assigned as $\rho = 2800$ kg/m^3.

Table 1: Assumed material properties of aluminium

Modulus of Elasticity, E	Poisson's Ratio, ν	Density, ρ
72000MPa	0.3	2800 kg/m^3

The full FE model of the simplified aircraft has 231,849 nodes, and it is computationally expensive to use all the nodes to identify the most suitable excitation point. This is because considering all possible input output FRFs would significantly increase the computational effort. To address this computational issue, the number of nodes was carefully reduced so that the selected nodes remain sufficient to represent all vibration modes required for the study. Therefore, 46 practical excitation and measurement nodes were carefully selected and renumbered in the FE model, as shown in Figure 2.

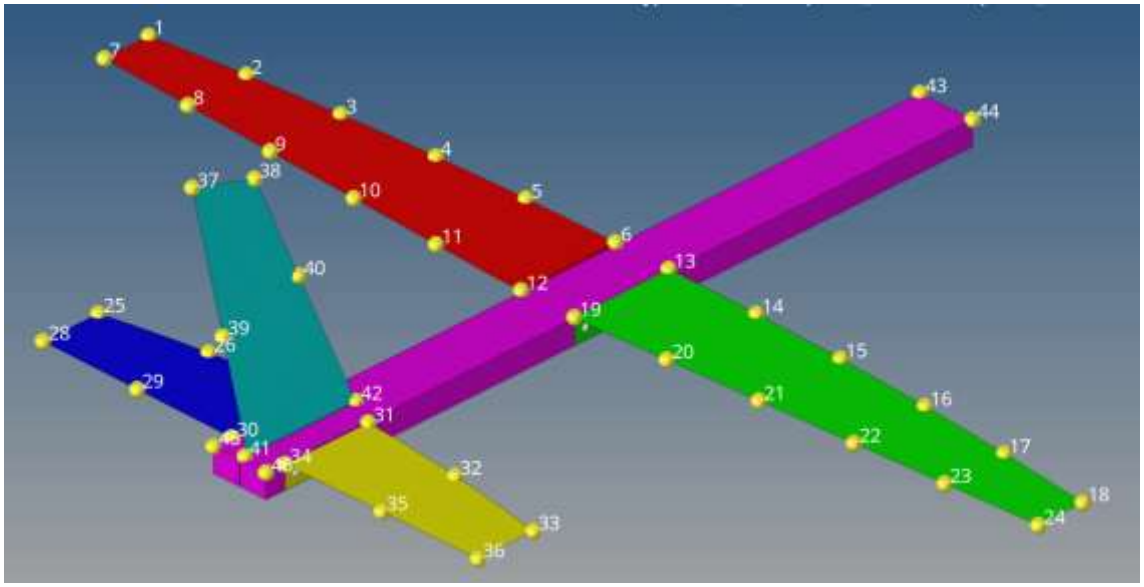

Figure 2: Practical excitation and measurement nodes required

Candidate Excitation Node Set

Although the full FE model consisted of 231,849 nodes, however, only 46 practical nodes (Figure 2) were selected for excitation node evaluation. The eigenvalues and eigenvectors of the full FE model were first obtained using MSC NASTRAN SOL103. The modal components associated with the retained modes within 0 to 150 Hz were subsequently extracted at the 46 nodes for modal participation factor analysis and excitation point ranking.

Equations of the Methodology

The eigenvalues and eigenvectors of the simplified aircraft are first obtained through modal analysis using MSC NASTRAN SOL103. The governing eigenvalue problem is expressed as

$$\left(\mathbf{K}-\omega_i^2\mathbf{M}\right)\phi_i=0 \tag{1}$$

where $\mathbf{M}$ indicates the global mass matrix, $\mathbf{K}$ is the global stiffness matrix, ω_i is the natural frequency of the mode and ϕ_i is the corresponding mode shape vector.

The extracted eigensolutions are subsequently used to calculate MPFs, which quantifies how effectively an external force applied at a particular node excites a particular mode. For mass normalised mode shape, the MPF is given by

$$\Gamma_i=\phi_i^T\mathbf{M}\mathbf{r} \tag{2}$$

where Γ_i indicates the modal participation factor, ϕ_i is the mode shape vector, $\mathbf{r}$ is the excitation director vector and $\mathbf{M}$ is the mass matrix.

The corresponding effective modal mass can be cast as

$$M_{\text{eff},i}=\Gamma_i^2 \tag{3}$$

or more generally,

$$M_{\text{eff},i}=\frac{\left(\phi_i^T\mathbf{M}\mathbf{r}\right)^2}{\phi_i^T\mathbf{M}\phi_i} \tag{4}$$

the effective modal mass ratio is then calculated as

$$\eta_i=\frac{M_{\text{eff},i}}{M_{\text{total}}}\otimes 100 \tag{5}$$

where the total participating mass is

$$M_{\text{total}}=\mathbf{r}^T\mathbf{M}\mathbf{r} \tag{6}$$

A large value of η_i indicates that the excitation point is highly effective in exciting the corresponding vibration mode.

To identify the most suitable excitation node, an excitation score is assigned to each candidate node j according to

$$Score_j=\sum_{i-1}^{N} w_i M_{\text{eff},ij} \tag{7}$$

where N is the number of modes considered, w_i is the modal weighting factor and $M_{\text{eff},ij}$ is the effective modal mass of mode i at candidate node j. The node with the highest score is expected to excite the largest number of modes within the frequency range of interest.

The selected excitation nodes are subsequently verified using MSC NASTRAN SOL111. Thee governing dynamic equation in the frequency domain is

$$\left(-\omega^2\mathbf{M} + j\omega\mathbf{C} + \mathbf{K}\right)\mathbf{X}(\omega) = \mathbf{F}(\omega) \tag{8}$$

where $\mathbf{C}$ is the damping matrix, $\mathbf{X}(\omega)$ is the response vector and $\mathbf{F}(\omega)$ is the excitation vector.

For a driving point FRF, where the excitation and response are measured at the same degree of freedom, the receptance FRF is defined as

$$H_{jj}(\omega) = \frac{X_j(\omega)}{F_j(\omega)} \tag{9}$$

where j denotes the response and excitation degree of freedom.

Using modal superposition, the general modal FRF between response node j and excitation node k is expressed as

$$H_{jk}(\omega) = \sum_{i=1}^{N} \frac{\phi_{ji}\phi_{ki}}{\omega_i^2 - \omega^2 + j2\zeta_i\omega_i\omega} \tag{10}$$

where ϕ_{ji} denotes the modal displacement at the response node, ϕ_{ki} is the modal displacement at the excitation node and ζ_i is the modal damping ratio of the i^{th} mode.

For a driving point FRF, where the excitation and response occur at the same node ($j = k$), Equation (10) simplifies to

$$H_{jj}(\omega) = \sum_{i=1}^{N} \frac{\phi_{ji}^2}{\omega_i^2 - \omega^2 + j2\zeta_i\omega_i\omega} \tag{11}$$

Equation (10) shows that the contribution of each mode to the driving point FRF is proportional to the square of the modal displacement at the excitation node. Consequently, excitation nodes associated with large modal amplitudes across multiple modes are expected to produce significant resonance peaks and provide more information on FRFs.

RESULTS AND DISCUSSION

This section presents and discusses the results obtained from normal modes, MPF, and FRF analyses used to evaluate the effectiveness of the proposed excitation point selection methodology for the simplified aircraft.

Excitation point selection using MPFs

Table 3 presents the excitation point ranking determined from the MPF and effective modal mass analysis for all candidate nodes considered in the FE model of the simplified aircraft (Figure 2). The scores are determined using Equation (7), where the contribution of each mode is evaluated based on the corresponding effective mass. In other words, nodes with larger scores highlight stronger modal controllability and greater capability to excite multiple structural modes within the frequency range of interest.

The results show that nodes 7, 24, 1 and 18 exhibit the highest excitation scores, indicating that these locations possess significantly larger modal participation contributions compared to the remaining candidate nodes. Based on Equations (2) to (5), large MPF and effective modal mass values are obtained when the modal displacement at the excitation location is large. Physically, this indicates that the selected excitation point is located away from modal nodal regions and is capable of efficiently coupling the external excitation force into the structural vibration modes.

In contrast, nodes 37 to 42 show substantially lower excitation scores, suggesting weak modal controllability at these locations. The low scores indicate that the corresponding mode shape amplitudes at these nodes are relatively small for most modes considered. Consequently, excitation at these locations is expected to generate weaker resonance responses and reduced modal visibility in the frequency response functions.

The excitation ranking results can also be interpreted using the modal form of the driving point FRF given in Equation (11). Since the modal contribution to the driving point FRF is proportional to the squared modal displacement term, nodes with larger modal amplitudes across multiple modes are expected to produce stronger resonance peaks and more information-rich FRFs. Therefore, the high ranking nodes identified in Table 3 are expected to provide improved excitation effectiveness during experimental modal analysis.

The MPF based ranking further demonstrates that excitation point selection cannot be determined solely based on geometric considerations. Instead, the dynamic characteristics of the structure, represented by the mode shapes and modal participation behaviour, must be considered to ensure sufficient excitation of the structural modes within the frequency range of interest.

Based on the obtained results, node 7 is identified as the most suitable excitation location due to its highest excitation score and strong modal participation contributions across multiple modes. Therefore, node 7 was selected for subsequent SOL111 frequency response analysis to verify the excitation effectiveness predicted by the MPF methodology.

Table 3: Ranking of candidate excitation nodes using MPF

Node	Score	Node	Score	Node	Score	Node	Score
7	669898.41	2	255473.75	35	44890.60	13	2251.87
24	669889.00	17	255468.47	29	44888.11	6	2250.38
1	657411.59	8	253873.68	32	43697.71	43	2248.80
18	657397.62	23	253864.77	26	43697.08	44	2244.78
36	380595.59	4	214550.57	34	2404.18	37	265.80
28	380591.91	15	214549.49	30	2396.42	39	242.02
33	364006.11	10	212296.20	46	2360.56	41	225.84
25	364005.85	21	212290.91	45	2352.59	38	218.98
22	289987.31	5	103897.26	31	2351.59	40	189.54
9	288546.09	14	103892.99	27	2345.08	42	155.77
3	286886.65	20	100557.88	19	2268.11		
16	286884.08	11	100549.59	12	2264.96		

Figure 3 compares the driving point FRFs obtained from several candidate excitation nodes (Figure 2) with different MPF ranking scores. The results show that the excitation location significantly influences the response amplitude and modal visibility of the structure. Nodes 7 and 33 exhibit substantially larger FRF amplitudes and clearer resonance peaks throughout the investigated frequency range, indicating strong modal controllability and effective excitation of multiple structural modes.

In contrast, nodes 37 and 42 generate considerably weaker FRF responses with reduced resonance visibility. Several resonance peaks become difficult to distinguish due to the small modal participation contributions at these locations. This behaviour suggests that these nodes are located close to modal nodal regions for many vibration modes, resulting in poor excitation effectiveness

The strong agreement between the MPF ranking results and the corresponding FRF responses demonstrates the effectiveness of the proposed MPF-based excitation point selection methodology.

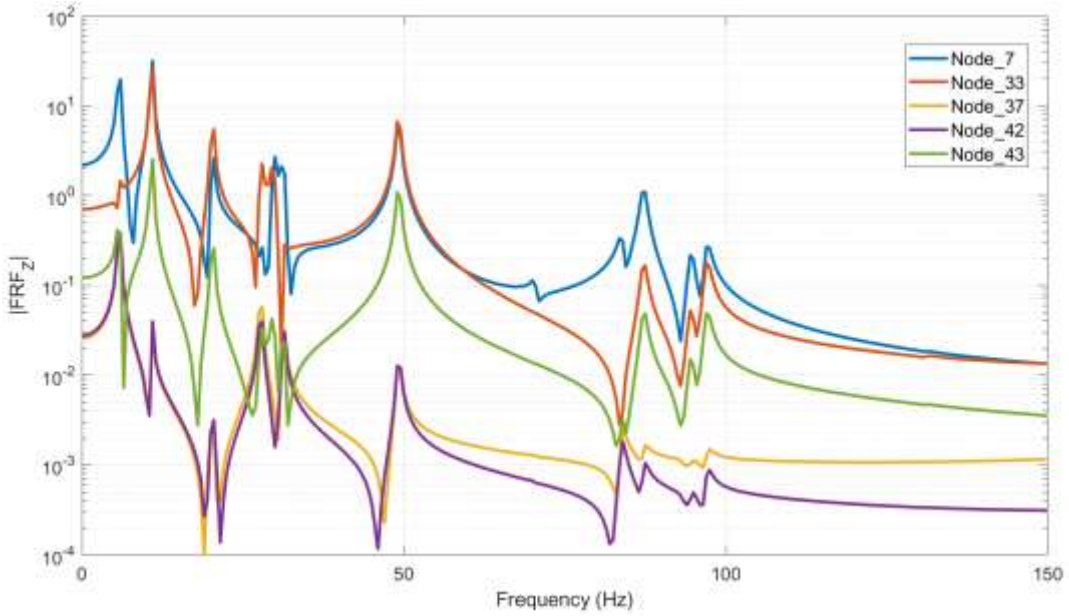

Figure 3: Comparison of driving point FRFs for different candidate excitation nodes

CONCLUSIONS

This study presents an MPF based methodology for identifying suitable excitation nodes for the simplified aircraft structure using MSC NASTRAN SOL103 and SOL111. The proposed approach successfully evaluates the modal contribution of candidate excitation nodes based on effective modal mass and MPFs.

The obtained results show that excitation nodes with large MPF and effective modal mass values exhibit significantly stronger driving point FRF and clearer resonance peaks across multiple vibration modes. In contrast, nodes with low MPF scores produce weak responses and reduced modal visibility, thereby indicating poor excitation effectiveness. The FRFs show strong agreement with the MPF based excitation ranking, thereby confirming the effectiveness of the proposed methodology.

The study further demonstrates that excitation point selection should not rely merely on geometric considerations but must account for the dynamic characteristics of the structure under study. The proposed methodology provides a systematic and efficient approach for identifying useful information excitation nodes for experimental modal analysis and structural dynamic investigations.

ACKNOWLEDGEMENTS

This study was conducted at the Structural Dynamics Analysis & Validation (SDAV) Laboratory, Faculty of Mechanical Engineering, Universiti Teknologi MARA (UiTM). The authors would like to express their gratitude to the SDAV team members for their technical support.

REFERENCES

[1] S.-E. Mir-Haidari and K. Behdinan, "Nonlinear effects of bolted flange connections in aeroengine casing assemblies," *Mechanical Systems and Signal Processing,* vol. 166, p. 108433, 2022/03/01/ 2022, doi: https://doi.org/10.1016/j.ymssp.2021.108433.

[2] R. Omar, M. A. Rani, and M. Yunus, "Representation of bolted joints in a structure using finite element modelling and model updating," *Journal of Mechanical Engineering and Sciences,* vol. 14, no. 3, pp. 7141 - 7151, %09/%30 2020, doi: 10.15282/jmes.14.3.2020.15.0560.

[3] C. Li, Y. Jiang, R. Qiao, and X. Miao, "Modeling and parameters identification of the connection interface of bolted joints based on an improved micro-slip model," *Mechanical Systems and Signal Processing,* vol. 153, p. 107514, 2021/05/15/ 2021, doi: https://doi.org/10.1016/j.ymssp.2020.107514.

[4] N. Karami, K. Jahani, and M. M. Ettefagh, "Investigation of Bolted Joint Modeling in a Horizontal Axis Wind Turbine Blade: Implications for Dynamic Analysis," *Journal of Vibration Engineering & Technologies,* vol. 13, no. 5, p. 348, 2025/06/04 2025, doi: 10.1007/s42417-025-01922-6.

[5] F. T. M. Kreutz, D.J. Rixen, "On the experimental linear identification of a multiple-joint bolted connection using frequency-based substructuring," presented at the Conference: ISMA 2024, Leuven, Belgium, 2024.

[6] H. Wemming, S. B. Lindström, L. Johansson, and Z. Kapidžić, "Modelling and experimental parameter identification for fasteners in composite–aluminium bolted structures," *Composite structures*, vol. 323, p. 117464, 2023.
[7] D. J. Ewins, *Modal Testing: Theory, Practice and Application*. Wiley, 2000.
[8] N. M. M. Maia and J. M. M. Silva, *Theoretical and Experimental Modal Analysis*. Research Studies Press, 1997.
[9] W. Heylen, S. Lammens, and P. Sas, *Modal analysis theory and testing* (no. 7). Katholieke Universiteit Leuven Leuven, Belgium, 1997.
[10] N. M. M. Maia *et al.*, *Structural Dynamics in Engineering Design*. Wiley, 2024.
[11] R. Allemang and P. Avitabile, *Handbook of Experimental Structural Dynamics*. Springer New York, 2022.
[12] K. Worden, *Nonlinearity in structural dynamics: detection, identification and modelling*. CRC Press, 2019.
[13] M. S. A. Mohd Kahar, W. I. I. Wan Iskandar Mirza, M. N. Abdul Rani, and M. A. Yunus, "Finite element modelling for the dynamic behaviour analysis of a structure with Hi-Lok fasteners," *Journal of Mechanical Engineering (JMechE)*, vol. 21, no. 3, pp. 231-246, 2024. [Online]. Available: https://ir.uitm.edu.my/id/eprint/101338/.
[14] J. Li, K. Lin, Y. Hu, Y. Yang, Y. Wang, and Z. Huang, "Multiple Impact Phenomenon in Impact Hammer Testing: Theoretical Analysis and Numerical Simulation," *Acta Mechanica Solida Sinica*, vol. 34, no. 6, pp. 830-843, 2021/12/01 2021, doi: 10.1007/s10338-021-00248-6.
[15] P. Li, W. Li, P. Wei, and Q. Wang, "Research on finite element analysis and modelling of bolted joint," *IOP Conference Series: Materials Science and Engineering*, vol. 892, no. 1, p. 012084, 2020/07/01 2020, doi: 10.1088/1757-899X/892/1/012084.
[16] S. Shokrollahi and F. Adel, "Finite element model updating of bolted lap joints implementing identification of joint affected region parameters," 2016.
[17] J. Maierhofer, A. E. Mahmoudi, and D. J. Rixen, "Development of a Low Cost Automatic Modal Hammer for Applications in Substructuring," in *Dynamic Substructures, Volume 4*, Cham, A. Linderholt, M. S. Allen, R. L. Mayes, and D. Rixen, Eds., 2020// 2020: Springer International Publishing, pp. 77-86.
[18] G. Kerschen, *Nonlinear Dynamics, Volume 1: Proceedings of the 36th IMAC, A Conference and Exposition on Structural Dynamics 2018*. CRC Press, 2025.